System Level Analysis of Multi-Operator Small Cell Network at 10 GHz

Petri Luoto*, Antti Roivainen†, Mehdi Bennis*, Pekka Pirinen*, Sumudu Samarakoon* Matti Latva-aho*
*Centre for Wireless Communications
University of Oulu, Finland
P.O. Box 4500, FI-90014 Oulu
{petri.luoto,mehdi.bennis,pekka.pirinen,
sumudu.samarakoon, matti.latva-aho}@oulu.fi

†Keysight Technologies Finland Oy
Tutkijantie 6,
FI-90590 Oulu
antti.roivainen@keysight.com

***Abstract*—Due to higher cost and spectrum scarcity, it is expected that an efficient use of spectrum in fifth generation (5G) networks will rather rely on sharing than exclusive licenses, especially when higher frequency allocations are considered. In this paper, the performance of a dense indoor multi-operator small cell network at 10 GHz is analyzed. The main goal is to show the benefits obtained at higher carrier frequency due to network densification while mobile network operators are sharing the spectrum. The analysis is assessed through extensive system level simulations. The main performance metrics are user throughput and signal-to-interference-and-noise ratio. Results show that when 10 GHz carrier frequency is used it allows higher network densities while satisfying user throughput requirements. However, when network is sparse lower carrier frequency leads to better performance. When network is dense, on average 2 Mb/s better mean throughput is achieved at 10 GHz when compared to traditional cellular frequency.**

***Index Terms*—channel, co-primary spectrum sharing, dense indoor, performance analysis, simulations, 5G.**

I. Introduction

From the current mobile communication system operating at frequency range below 6 GHz, it cannot be expected to provide sufficient data rates in the future fifth generation (5G) mobile communication system. Radio frequencies above 6 GHz have the potential to allow wider bandwidths and thus, higher data rates than licensed mobile communication system operating below 6 GHz. Therefore, 5G mobile communication system will rely on the higher frequency allocations.

Co-Primary Spectrum Sharing (CoPSS) is one possible spectrum sharing technique towards 5G systems, where any mobile network operator (MNO) is allowed to utilize the shared spectrum allocated for 5G cellular systems [1]. In [2], CoPSS is defined as a spectrum access model where primary license holders agree on the joint use of (or parts of) their licensed spectrum. Depending on the carrier frequency, spectrum requirements will include: large chunks of the spectrum in higher frequency bands and a flexible use of spectrum through advanced spectrum sharing techniques [3].

The properties of channel at different frequency bands might have significant effect on the spectrum sharing techniques. For example, higher path loss indicates the lower strength of desired signal. On the other hand, the strengths of interfering signals decrease as well. In this paper, we analyze indoor spectrum sharing techniques at 10 GHz. According to the authors' best knowledge spectrum sharing techniques via extensive Monte Carlo type of system level simulation studies have not been performed at 10 GHz in the existing literature. Furthermore, we compare the performance of the algorithms against the currently licensed spectrum at 2 GHz and analyze the potential of using 10 GHz carrier frequency for spectrum sharing.

In order to study different frequency spectrum sharing techniques, the core of the extensive LTE-A system level network simulator has been built according to the International Telecommunication Union's system level simulation guidelines [4] utilizing WINNER II channel model implementation [5] and parametrization [6]. In [7], [8], the simulator has been calibrated and rigorously evaluated in selected macrocell and microcell environments at 2 GHz. Moreover, the simulator has been extended to incorporate indoor femtocells, calibrated and verified in [9] and utilized in [10], [11].

This paper is organized as follows. The link and system model is defined in Section II. In Section III, describes shortly the actual CoPSS algorithms and the main differences between propagation channel at 2 GHz and 10 GHz. Section IV provides numerical results of the CoPSS algorithms at 10 GHz and comparison to 2 GHz carrier frequency. Finally, Section V concludes the paper.

II. Link and System Models

Consider the downlink of an Orthogonal Frequency-Division Multiple Access (OFDMA) small cell network (SCN) where a set of SCNs $\mathcal{B}$, operated by a set of MNOs $\mathcal{L} = \{1, \cdots, l\}$, are deployed. MNO l controls a set of its own SCNs $\mathcal{B}_l$, and thus $\mathcal{B} = \cup_{\forall l \in \mathcal{L}} \mathcal{B}_l$ with $\mathcal{B}_l \cap \mathcal{B}_{l'} = \emptyset$ for all

This research was supported by the Finnish Funding Agency for Technology and Innovation (Tekes), Nokia, Anite, Huawei Technologies, and Infotech Oulu Graduate School. Kari Horneman and Ling Yu, from Nokia earn special thanks for invaluable guidance for this study.

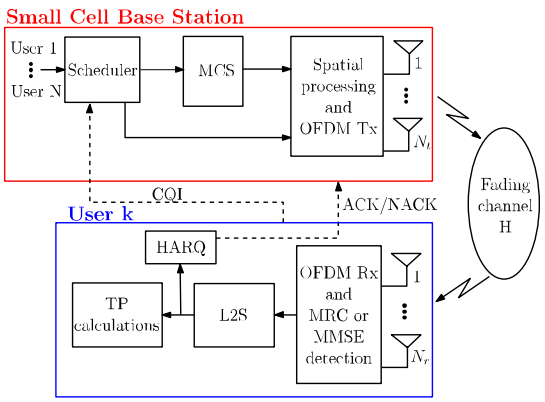

Fig. 1: Block diagram of the link model.

$l \neq l'$. Each SCN $b \in \mathcal{B}$ has K users. The frequency domain resource consists of N_c subcarriers, where 12 subcarriers form a physical resource block (PRB) and 6 PRBs form a component carrier (CC). A common pool consists of N_{cc} number of CCs. It is assumed that the spectral allocations of the SCNs are orthogonal to the macrocell network layer, and thus only the small cell traffic is modeled. Moreover, we assume that SCNs do not coordinate with each other.

The link model between a SCN and a user is illustrated in Fig. 1. A link-to-system (L2S) interface is used in the simulations. Each user is paired to the SCN based on the path loss model [12], [13]. A geometry-based stochastic channel model (GSCM) [6], [14] is used to model fast fading and shadowing losses for all links. Channel parameters are determined stochastically, based on the statistical distributions extracted from channel measurements [6]. However, SCN related assumptions for the links and channel parameters are adopted from [12]: all links are assumed to be non-line-of-sight (NLOS) and users are always inside buildings.

User k estimates channel-quality indicator (CQI) information, i.e., quantized signal-to-interference-plus-noise ratio (SINR), from the received signal for every CC and send it to the SCN. The uplink channel is assumed to be ideal, i.e., error free. Errors are considered in the receiver side. However, in order to model a practical closed loop system, periodic and delayed CQI is assumed. At SCN, the proportional fair scheduler utilizes the CQI information in the allocation of frequency resources to the most suitable users. After scheduling, the link adaptation is performed for scheduled users by selecting modulation and coding scheme (MCS) based on CQI information. Finally, the data is sent over the fading channel. The cyclic prefix is assumed to be longer than the multipath delay spread, and thus inter-symbol-interference is not considered.

At the receiver, perfect frequency and time synchronization is assumed. Link-to-system mapping is performed using mutual information effective SINR mapping (MIESM) [15]. This significantly reduces the computational overhead in comparison to the exact modeling of the radio links, while still providing sufficiently accurate results. In the L2S interface, SINR is calculated and mapped to corresponding average mutual information. Based on the MIESM value, the frame error probability (FEP) is approximated according to a predefined frame error rate (FER) curve of the used MCS. Based on the FER, successful and erroneous frames can be detected, and hybrid automatic repeat request (HARQ) can take the control of retransmissions. An acknowledgement (ACK) or a negative acknowledgement (NACK) message is sent back to the SCN to signal the success or failure of the transmission, respectively. The results are obtained by simulating a predefined number of channel samples.

III. Co-Primary Spectrum Sharing Algorithms and Channel Model

A. Spectrum Sharing Algorithms

Since the main objective in this paper is to study spectrum sharing techniques at 10 GHz in indoor scenario, the used algorithms and solvable problem are shortly described. The problem formulation and used algorithms are described in more detail in [11].

We consider a CoPSS-enabled system where each MNO has its own dedicated spectrum and has access to the shared common pool of CCs as shown in Fig. 2. The main goal is to achieve a target rate per SCN b.

The performance of multi-operator small cell network is evaluated with three spectrum sharing algorithms: two state-of-art algorithms (Equal and Greedy) and a decentralized algorithm (Gibbs) proposed in authors' former work [11]. Here, we shortly describe the used spectrum sharing algorithms:

- *Equal:* The common pool of CCs is shared orthogonally and equally between MNOs. This algorithm performs well in scenarios where SCNs are colocated. In such scenarios, the SCNs are close to each other and thus, the serving signal and the interference signal would have approximately the same strength, leading to a high FER. Therefore, it is crucial that simultaneous use of the shared CCs is avoided.
- *Greedy:* The second algorithm is a greedy (decentralized) algorithm, where each SCN selects suitable set of CCs in a greedy manner. The main goal is to achieve the target rate. Thus, fairness among MNOs cannot be guaranteed.
- *Gibbs+penalty:* The third algorithm is proposed in [11] which is a reinforcement learning mechanism based on Gibbs sampling [16]. Here, each SCN autonomously selects a suitable set of CCs, $x_b(t)$, to minimize their cost functions in a decentralized manner. This learning algorithm provides a mechanism to choose $x_b(t)$ at each time instant t with a given probability that depends on the estimated average rate.

B. Channel Model

In the GSCM, propagation channel is characterized by statistical parameters obtained from the radio channel measurements. This gives a possibility to use the same framework of the model for the simulations in different frequencies and the different number or types of antennas. At 10 GHz, the

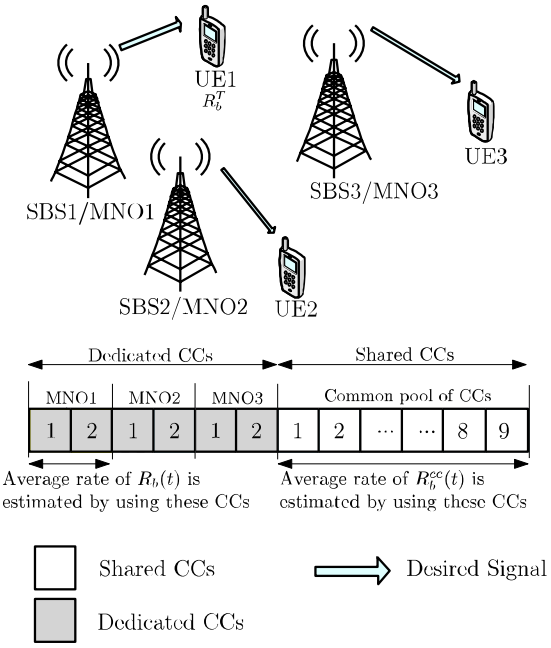

Fig. 2: System model and spectrum allocation.

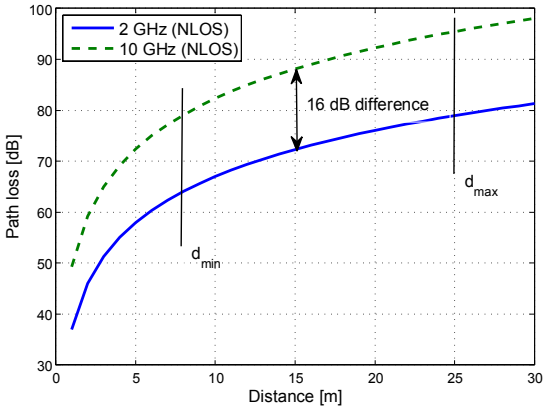

Fig. 3: Path loss (NLOS) comparison between 2 GHz and 10 GHz.

statistical parameters of the model have been derived from the experimental channel measurements, and presented in [13]. Statistical parameters at 2 GHz have been taken from [6]. Both of the measurements has been carried out in similar environment.

Radio propagation channel behaves differently at different frequency bands. In general, path loss (PL) increases as the carrier frequency increases. However, due to shorter wavelength at 10 GHz, more antenna elements can be filled into the same space, making room to high gain antenna arrays to mitigate the increased path loss. Considering other channel model parameters at 10 GHz, the second order statistics, for example, delay spread and the angle spreads are smaller due to higher attenuation of multipath components [13] in comparison to corresponding parameters at lower frequency band in [6].

Path loss models for indoor NLOS scenario at 2 GHz and 10 GHz are given by:

$$\mathrm{PL}_{@2\mathrm{GHz}} = 30\log_{10}(d) + 37 + A_{\mathrm{in}}n, \quad (1)$$

and

$$\mathrm{PL}_{@10\mathrm{GHz}} = 33\log_{10}(d) + 49.3 + A_{\mathrm{in}}n, \quad (2)$$

respectively. In (1) and (2) d is distance in meters, A_{in} is the penetration loss of internal wall, and n is the number of penetrated walls. In general, the construction materials of the wall have significant impact on the penetration loss. Due to lack of internal wall penetration loss results at 10 GHz, we use the penetration loss of 10 dB for each internal wall at the higher frequency band.

Fig. 3 compares the path losses at 2 GHz and 10 GHz as a function of distance. In Fig. 3, d_{min} and d_{max} are the minimum and maximum distances between SCN and user in the simulations. Fig. 3 shows that there is 16 dB larger path loss for the higher carrier frequency.

IV. System Level Analysis

System level simulations are particularly useful for studying network related issues, such as resource allocation, interference management and mobility management. In this work, a multi-operator LTE-A system level simulator is used to model a cellular network consisting of an indoor SCN with multiple operators. Moreover, 5G related system level simulations are also necessary in the future because we can not only rely on analytical analysis. Furthermore, when the simulation platform follows the standardization it can provide reliable results on the expected performance.

A. Simulator Layout and Parameters

The simulator uses a layout that has a building of size 120 m $\times$ 120 m. The building has one open corridor across it and in total 20 rooms, size 24 m $\times$ 24 m as shown in Fig. 4, which can be modeled an office environment, a shopping mall, an apartment, etc. Internal wall attenuation is 5 dB and 10 dB per wall, at 2 GHz and 10 GHz, respectively. SCNs are randomly distributed, the number of SCNs in the building is based on deployment probability η, e.g., the probability that one room has an SCN. SCNs are uniformly distributed in the rooms. Maximum number of SCNs in the building is 25, corridor is considered as five blocks without walls. Users are evenly distributed and each of them is connected to own MNO's SCN. A single user is connected to each SCN. Traffic in the network is constant and each user/MNO has a target rate of 15 Mb/s. Table I summarizes the main simulation parameters and assumptions which are used in simulations.

B. Performance Comparison Results

The mean received SINR of the two carrier frequencies and CoPSS algorithms are analyzed in Fig. 5. First, we can see that the received SINR is smaller at 10 GHz carrier

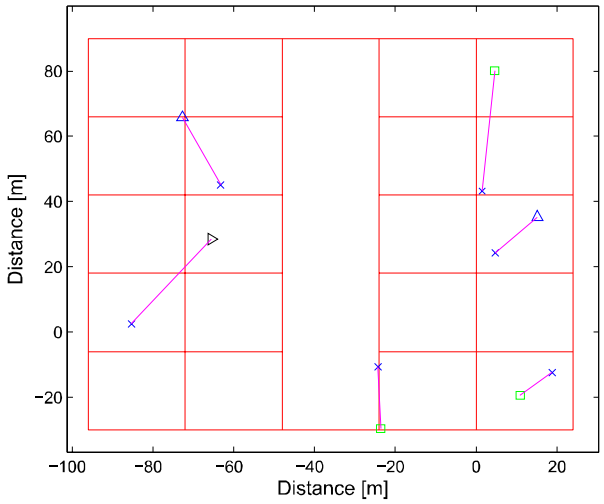

Fig. 4: Small cell layout where base stations are randomly located. Blue triangle, black triangle, and green square denotes SCN for different MNOs, while blue cross indicates user. Line between user and SCN shows the radio link.

TABLE I: Simulator parameters and assumptions.

Parameter	**Assumption**
Transmission direction	Downlink
Duplex mode	FDD
System bandwidth	20 MHz
Number of CCs	2 per MNO
Number of CCs common pool	9
Number of users	1 user per SCN
Antenna configurations [Tx × Rx]	1 × 2
Receiver	maximum ratio combining
HARQ	Chase combining
SCN transmission power	20 dBm
Feedback CQI period	6 ms
Feedback CQI delay	2 ms
Traffic model	Continuous constant rate transmission
Internal wall attenuation A_{in}	5 dB at 2 GHz, 10 dB at 10 GHz

frequency, especially when SCN deployment probability η is low. The main reason is the higher path loss at 10 GHz. When η is increased, received SINR at 2 GHz carrier frequency decreases about 20 dB, while at 10 GHz, the decrease is only 10 dB. The reason is that the number of interfering SCNs in a dense network is much lower at higher carrier frequency in comparison to the lower carrier frequency due to the higher path loss. From spectrum sharing point of view, Gibbs algorithm is providing good SINR while the SINR of Greedy algorithm decreases rapidly as η increases. The reason is that Gibbs algorithm learns suitable set of CCs in which the interference is minimized.

Next, in Fig. 6, we show the achieved mean throughput for two carrier frequencies and CoPSS algorithms. These results show that we can achieve higher throughput when the higher carrier frequency is used especially when the network is dense, even though, the previous figure indicated that received SINR

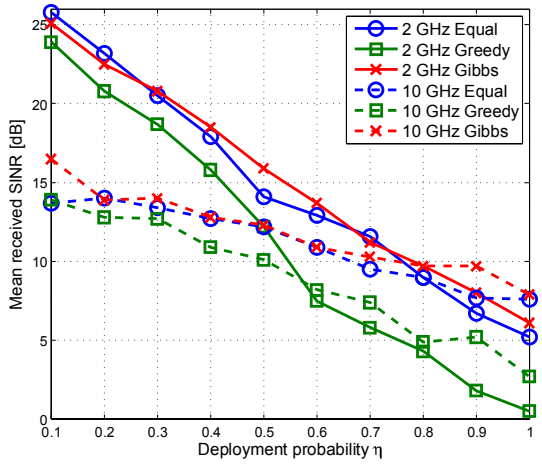

,

Fig. 5: Mean received SINR for different CoPSS algorithms and carrier frequencies when deployment probability is increased.

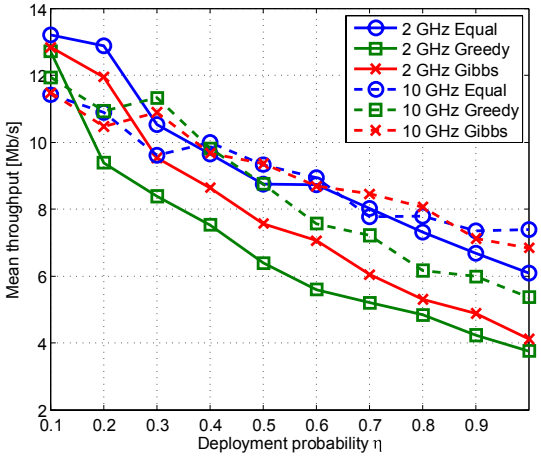

Fig. 6: Mean throughput for different CoPSS algorithms and carrier frequencies when deployment probability is increased.

is lower. The main reason is that the received SINR is not directly mapped to the achieved throughput (MIESM is used). Furthermore, the allocated resources can vary when different carrier frequencies are used. The achieved performance with Equal algorithm is somewhat similar with both carrier frequencies because of the fixed spectrum allocation.

In Fig. 7, cumulative distribution function (CDF) of the throughput is analyzed when SCN deployment probability is 50 %. At 10 GHz, the best overall performance is achieved. With the higher carrier frequency, the cell edge performance (5% from CDFs) is improved. Especially when Gibbs algorithm is used, cell edge throughput is improved up to 1.3Mb/s.

Table II summarizes the achievable cell edge users' (5% from CDFs) throughputs. Table shows that when carrier frequency is increased cell edge throughput is increased. Further-

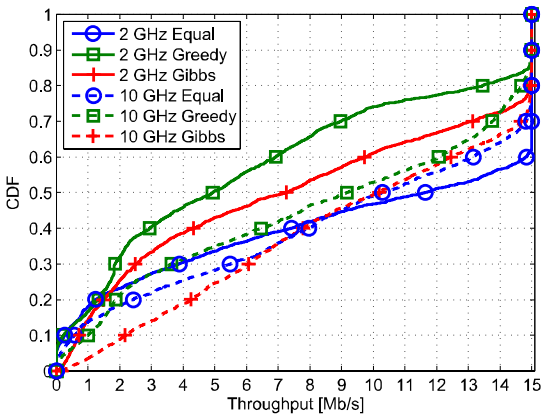

Fig. 7: CDF of downlink user throughput for different CoPSS algorithms and carrier frequencies when target rate is 15 Mb/s, and SCN deployment probability is 50 %.

TABLE II: Cell edge user throughput for different deployment probabilities, carrier frequencies, and CoPSS algorithms.

	$\eta = 10\%$		$\eta = 50\%$		$\eta = 100\%$	
	2 GHz	10 GHz	2 GHz	10 GHz	2 GHz	10 GHz
Equal	1.1	2.2	–	0.13	–	–
Greedy	1.9	1.8	–	0.33	–	–
Gibbs	5.5	2.7	0.6	1.2	0.1	1.3

more, when $\eta = 100\%$, Equal and Greedy algorithms are in outage and only Gibbs algorithm provides throughput of 1.3 Mb/s at 10 GHz.

Analyzing all the results together, we can conclude that higher carrier frequency can provide better performance and it allows denser networks. The CoPSS algorithm proposed in [11] is the best one and the performance is even better at higher carrier frequency.

V. Conclusion

We have evaluated indoor small cell co-primary multi-operator spectrum sharing environment at 10 GHz and compared it to the traditional cellular frequency at 2 GHz. The framework has been established under the LTE-A compliant system simulation platform where the system throughput performance and signal-to-interference-plus-noise ratio has been rigorously assessed. Provided numerical results confirm the possibility for network densification when higher carrier frequency is used and at the same time to further increase system throughput in the multi-operator setting when mobile network operators are sharing a common pool of component carriers. The results show that learning based algorithms without any coordination between small cell networks (SCNs) can be used in the spectrum sharing and especially when higher carrier frequency is used. In our future work, we will further increase the performance by including coordination among SCNs.

References

[1] "World Radiocommunication Conference 2015." [Online]. Available: http://www.itu.int/en/ITU-R/conferences/wrc/2015/

[2] "METIS deliverable D5.1 Intermediate description of the spectrum needs and usage principles." [Online]. Available: https://www.metis2020.com/wp-content/uploads/deliverables/METIS_D5.1_v1.pdf

[3] Nokia, "Looking ahead to 5G." [Online]. Available: http://networks.nokia.com/sites/default/files/document/5g_white_paper_0.pdf

[4] "Guidelines for evaluation of radio interface technologies for IMT-Advanced, Report ITU-R M.2135-1, 2009."

[5] "MATLAB implementation of the WINNER Phase II Channel Model ver1.1." [Online]. Available: https://www.ist-winner.org/phase_2_model.html

[6] "WINNER II channel models, D1.1.2 V1.0." [Online]. Available: http://www.cept.org/files/1050/documents/winner2%20-%20final%20report.pdf

[7] H. Pennanen, T. Haataja, J. Leinonen, A. Tölli, and M. Latva-aho, "System level evaluation of TDD based LTE-Advanced MIMO-OFDMA systems," in *IEEE GLOBECOM Workshops (GC Wkshps)*, Dec. 2010, pp. 809–813.

[8] T. Haataja, H. Pennanen, J. Leinonen, A. Tölli, and M. Latva-aho, "Space-frequency scheduling in TDD based LTE-Advanced MIMO-OFDMA systems," in *IEEE 73rd Vehicular Technology Conference (VTC Spring)*, May 2011, pp. 1–5.

[9] "BeFEMTO." [Online]. Available: http://www.ict-befemto.eu/home.html

[10] P. Luoto, J. Leinonen, P. Pirinen, V. V. Phan, and M. Latva-aho, "Bitmap based resource partitioning in LTE-A femto deployment," in *IEEE International Conference on Communications (ICC)*, Jun. 2013, pp. 5005–5009.

[11] P. Luoto, M. Bennis, P. Pirinen, S. Samarakoon, and M. Latva-aho, "Gibbs sampling based spectrum sharing for multi-operator small cell networks," in *2015 IEEE International Conference on Communication Workshop (ICCW)*, Jun. 2015, pp. 967–972.

[12] "BeFEMTO. Assumptions For System Level Calibration. Version 0.8 March, 2011."

[13] A. Roivainen, C. Ferreira Dias, N. Tervo, V. Hovinen, M. Sonkki, and M. Latva-aho, "Geometry-based stochastic channel model for two-story lobby environment at 10 GHz," *IEEE Transactions on Antennas and Propagations.*, vol. 64, no. 9, pp. 3990–4003, Sep. 2016.

[14] "3rd Generation Partnership Project, Technical Specification Group Radio Access Network, Spatial channel model for Multiple Input Multiple Output (MIMO) simulations, 3GPP Technical report 25.996 v6.1.0, 2003."

[15] X. He, K. Niu, Z. He, and J. Lin, "Link layer abstraction in MIMO-OFDM system," in *International Workshop on Cross Layer Design (IWCLD)*, Sep. 2007, pp. 41 –44.

[16] L. P. Qian, Y. J. Zhang, and M. Chiang, "Distributed nonconvex power control using Gibbs sampling," *IEEE Trans. Commun.*, vol. 60, no. 12, pp. 3886–3898, 2012.